ACS OMEGA

http://pubs.acs.org/journal/acsodf

Article

On Degree-Based Topological Indices of Carbon Nanocones†

Karnika Sharma, Vijay Kumar Bhat,* and Sunny Kumar Sharma

Cite This: *ACS Omega* 2022, 7, 45562−45573

Read Online

ACCESS | Metrics & More | Article Recommendations

ABSTRACT: Topological descriptors are numerical numbers that are assigned to molecular structures and can predict certain physicochemical properties. Because of their importance in nanotechnology and as developing materials with practical uses, the topological properties of nanocones have received a lot of attention. In this paper, we discuss the ev-degree- and ve-degree-based topological indices for the generalized carbon nanocones, $CNC_r[s]$. Furthermore, we find numerical computations for certain types of nanocones and plot these numerical results using Matlab programming.

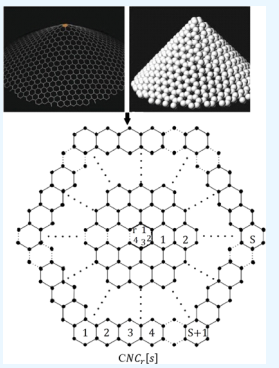

INTRODUCTION

Carbon nanocones first appeared on the surface of the naturally occurring graphite in 1968 or perhaps earlier.[1] The possible uses of these chemical structures in energy storage, gas storage, gas sensors, biosensors, nanoelectronic devices, and chemical probes are interesting.[2] Nanocones are carbon chains that can be mathematically described as infinite graphs of the cubic plane. The molecular graph of nanocones contains conical structures with a cycle of length q and p layers of hexagons arranged around its center shown in Figure 2. In ref 3, the presence of carbon nanocone and their combinational features were studied. Klein et al.[1] divided nanocones into eight groups based on the definite signed curvature. These structures have been categorized by Brinkmann et al.[4] The expander constants and boundaries of these nanocone triangular patches were determined by Justus et al.[5] Furthermore, carbon nanocones attracted the researchers' interest due to their unusual features and potential applications in a variety of new fields, including energy and hydrogen storage.[6]

The structural and computational properties of carbon nanocones have been the topic of several studies over the years,[7,8] many of which have been prompted by the introduction of such nanomaterials and fullerenes.[9] Mortazavi et al. motivated by the chemical vapor deposition experiment conducted extensive first-principles-based simulations to explore the stability, mechanical properties, lattice thermal conductivity, piezoelectric and flexoelectric response, and photocatalytic and electronic features of MA_2Z_4 (M = Cr, Mo, W; A = Si, Ge; Z = N, P) monolayers. Moreover, they obtained that among all two-dimensional (2D) materials, the monolayers of WSi_2N_4, $CrSi_2N_4$, and $MoSi_2N_4$ show the highest piezoelectric coefficients. They also found that the monolayers of $MoSi_2N_4$ and WSi_2N_4 exhibit high lattice thermal conductivity and mechanical strength. Additionally, these nanosheets are used in photocatalytic water splitting and optoelectronics.[10] Javvaji et al. found that the accurate examination of electricity generation stemming from higher-order deformation (flexoelectricity) in 2D layered materials is a highly challenging task, and to address this challenge, they proposed an innovative and computationally efficient approach on the basis of density functional theory (DFT) and machine-learning interatomic potentials (MLIPs) with incorporated long-range interactions to accurately investigate the flexoelectric energy conversion in 2D van der Waals bilayers. The studies of Jahanbani,[11] Zobair et al.,[12] and Arockiaraj et al.[13] contain the number of calculations for some specific topological indices of carbon nanocones based on distance. These studies also look at a range of topological indices that are calculated using diverse methods.

The topological index of a molecular structure can be thought of as a nonempirical numerical value that quantifies the molecular structure and its branching pattern. From this vantage point, the topological index can be seen as a score function that converts each chemical structure into a real number and serves as a description of the molecule being tested. The biggest factor behind the widespread attention paid

Received: September 29, 2022
Accepted: November 9, 2022
Published: December 2, 2022

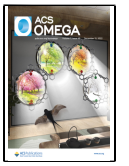

https://doi.org/10.1021/acsomega.2c06287
ACS Omega 2022, 7, 45562−45573

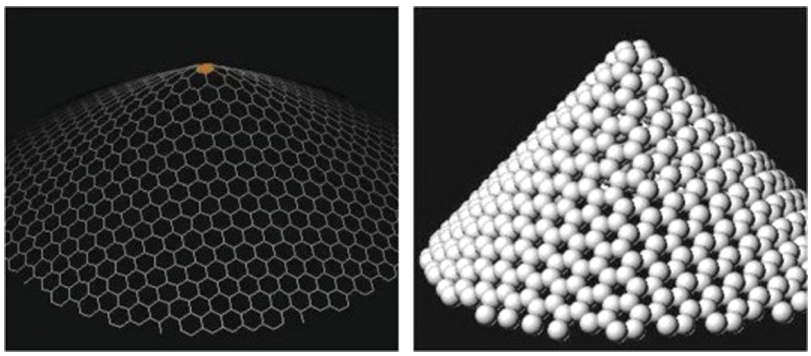

Figure 1. 3D structures of $CNC_r[s]$.

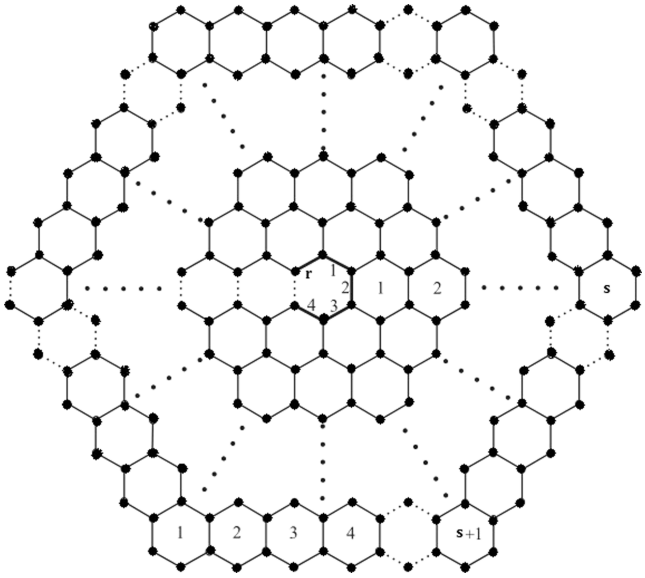

Figure 2. Generalized carbon nanocones, $CNC_r[s]$.

to these indices is the amazing ability to correlate and predict the characteristics of a wide variety of molecular structures. For example, these indices are utilized in the development of QSAR/QSPR relationships in which the thermodynamic properties (heats of formation and vaporization), physicochemical properties (boiling point, solubility, and refractive index), biophysical properties (bioconcentration factor, biodegradability, and soil sorption), and physiological properties of molecules (carcinogenicity and toxicity) are correlated and predicted with their molecular structures.[14] The fact is that the topological indices are actually graph invariants. This means that they define the properties of the hydrogen-suppressed graph of a molecule in terms of a mathematical equation that is independent of the graph's orientation and possible vertex-numbering scheme. When it comes to TIs, the expression takes on the form of a scalar descriptor with a number value.

In the literature to date, more than 100 unique TIs have been proposed, although only a considerably smaller number have been shown to be significant in correlative or predictive research. The first publication in the series[15] demonstrated how TIs could be used to forecast the sound velocity in various alkane and alcohol species. Then, an effort to correlate a threshold shoot index feature is frequently used to describe hydrocarbon fuels for the first time.[16] To have any graph properties, a molecule needs a definite number of atoms linked together in a specific configuration by relatively strong chemical bonds. Therefore, weakly defined or ephemeral chemical structures, such as intermediates, hydrogen-bonded species or species that interact significantly with their environment to produce charge-transfer complexes are not appropriate for characterization by TIs. Generally speaking, this means that the molecules under consideration must be clearly characterized as separate and unrelated entities that exist independently of their surroundings.

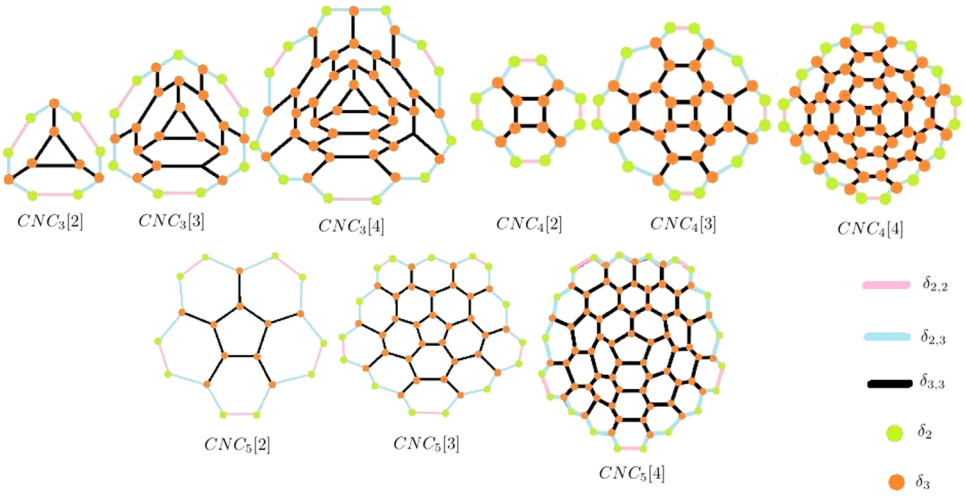

Figure 3. Molecular structures of $CNC_r[s]$ for $r = 3-5$ and $s = 2-4$.

https://doi.org/10.1021/acsomega.2c06287
ACS Omega 2022, 7, 45562−45573

In theoretical chemistry, molecular structures are represented as chemical graphs in which every vertex and edge represents an atom and bond between the two atoms of a molecular structure. Numerous studies show that there is a significant underlying relationship between the molecular structures of chemical compounds and their physical properties, such as boiling and melting points. To better comprehend the physical characteristics, chemical reactivity, and biological activity of these chemical molecular structures, topological indices have been established. Due to the absence of chemical experiments, the study of topological indices on the chemical structure of compounds can fill the gap and offer a scientific base for the production of a large number of new drugs and chemical compounds. However, the chemically based investigations showed that there was a high correlation between topological molecular structures and their physical properties, chemical characteristics, and biological factors, such as melting point, boiling temperature, and drug toxicity. For understanding the links between the molecular structure and possible physicochemical properties, chemical engineers use a number of well-known indices, such as the Wiener index, Zagreb index, Randic index, Harmonic index, etc.

Wiener[17] proposed the first distance-based topological index in 1947 while researching the boiling point of alkane molecules. Numerous categories, including degree-based, distance-based, and counting-based, have been used to classify topological indices.[18] Among these, topological indices based on degrees play an important role in theoretical chemistry and pharmacology. Degree-based topological indices have been actively investigated to examine the attributes of substances and medications as it is helpful to correct the experimental flaws in chemical and medicinal research. In QSAR/QSPR modeling,[19] degree-based topological indices are often used descriptors because of their simplicity in understanding, applicability, computation, and derivation without the need for any experimental work. We refer to refs 19−21 for additional degree-based topological indices that have been employed in QSAR/QSPR models. For forecasting the physical characteristics of alcanes, Platt proposed the first degree-based topological index in 1947.[22] In 1972, Gutman and Trinajstić[23] created and expanded the Zagreb indices, which have been used for more than 50 years.

Later, Zhong[24] described Harmonic index and afterward Ediz et al.[25] established the new Harmonic indices. The previous study, on the other hand, was completed using the conventional degree system. The vertex−edge domination and the edge−vertex domination characteristics were used by the researchers to create these innovative degree notions.[26,27] The concepts of vertex−edge domination and edge−vertex domination were introduced by Peters[26] in 1987. In the discipline of graph theory, Chellali et al.[28] developed two new degree ideas, ve-degree and ev-degree. Horoldagva et al.[29] also look at some of the computational ideas relating to ve-degree and ev-degree. The conventional degree-based principles were converted into ev- and ve-degree Randic indices, as well as ev- and ve-degree Zagreb indices, in ref 30. It has been proven that the ve-degree Zagreb index is more reliable than the conventional Zagreb index.

The Randic index has received more attention in chemical and mathematics literatures than any other topological indices. By simulating a few physicochemical characteristics of octane isomers, the ev-degree Randi index is contrasted with the Randic index. It has been demonstrated that the ev-degree Randi index correlates better than the Randic index to forecast the entropy, acentric factor, and standard enthalpy of octanes' vaporization.[30,31] In comparison to other well-known topological indices as Zagreb, Randic, atom−bond connectivity, and sum connectivity indices, it has been demonstrated that the ve-degree sum connectivity index of octane isomers provides the best value of correlation coefficient of the property of acentric factor.[32] The definition and examination of the fundamental mathematical features of the ev-degree and ve-degree topological indices have taken place in refs 29, 31.

In this study, we looked at a few ve-degree and ev-degree concepts. We provide the ve-degree- and ev-degree-based topological indices for the molecular structure of the carbon nanocone $CNC_r[s]$. Topological indices or variants based on ve-degree and ev-degree are currently the subject of a lot of research (see refs 33−38 for a more extensive explanation of these topological indices of several graphs and molecular structures). In this work, the second ve-degree Zagreb β-index ($M^{\beta}_{2,ve}$), ve-degree Randic index (R_{ve}), ev-degree Randic index (R_{ev}), ev-degree Zagreb index (M_{ev}), the first ve-degree Zagreb α-index ($M^{\alpha}_{1,ve}$), the first ve-degree Zagreb β-index ($M^{\beta}_{1,ve}$), ve-degree atom−bond connectivity index (ABC_{ve}), ve-degree sum connectivity index (χ_{ve}), ve-degree harmonic index (H_{ve}), and ve-degree geometric−arithmetic index (GA_{ve}) are examined for the molecular structure of carbon nanocone $CNC_r[s]$. Numerical computations and verification are also carried out using Matlab programming. Moreover, Matlab is also used to plot the numerical results.

Structures of Carbon Nanocones. In this work, Figure 1 depicts the three-dimensional (3D) structures of carbon nanocones and Figure 2 shows a molecular graph of generalized carbon nanocones $CNC_r[s]$, which consists of conical structures with a cycle of length r and s layers of hexagons positioned around the conical surface. In graph theory, a carbon nanocone is a graph having an r-cycle shape because its center is encircled by s layers of hexagons, with s hexagons on every outer side. The generalized carbon nanocones can be described as $CNC_r[s]$ for $r \geq 3$ and $s \geq 2$, as seen in Figure 3. Assuming, $\Gamma = CNC_r[s]$, the Γ contains rs^2 vertices and $\frac{rs}{2}(3s - 1)$ edges.

PRELIMINARIES

In this section, we define some basic concepts and the topological indices based on ev-degree and ve-degree (see Table 1).

Table 1. Topological Indices Formulas

ev-degree Zagreb index (M_{ev})	$M_{ev} = \sum_{e\in E}\Psi_{ev}(e)^2$
First ve-degree Zagreb α-index ($M^{\alpha}_{1,ve}$)	$M^{\alpha}_{1,ve} = \sum_{v\in\vartheta}\Psi_{ve}(v)^2$
First ve-degree Zagreb β-index ($M^{\beta}_{1,ve}$)	$M^{\beta}_{1,ve} = \sum_{uv\in E}(\Psi_{ve}(u) + \Psi_{ve}(v))$
Second ve-degree Zagreb β-index ($M^{\beta}_{2,ve}$)	$M^{\beta}_{2,ve} = \sum_{uv\in E}(\Psi_{ve}(u) \times \Psi_{ve}(v))$
ve-degree Randic index (R_{ve})	$R_{ve} = \sum_{uv\in E}(\Psi_{ve}(u) \times \Psi_{ve}(v))^{-1/2}$
ev-degree Randic index (R_{ev})	$R_{ev} = \sum_{e\in E}\Psi_{ev}(e)^{-1/2}$
ve-degree atom−bond connectivity index (ABC_{ve})	$ABC_{ve} = \sum_{uv\in E}\sqrt{\frac{\Psi_{ve}(u) + \Psi_{ve}(v) - 2}{\Psi_{ve}(u) \times \Psi_{ve}(v)}}$
ve-degree geometric−arithmetic index (GA_{ve})	$GA_{ve} = \sum_{uv\in E}\frac{2\sqrt{\Psi_{ve}(u) \times \Psi_{ve}(v)}}{\Psi_{ve}(u) + \Psi_{ve}(v)}$
ve-degree harmonic index (H_{ve})	$H_{ve} = \sum_{uv\in E}\frac{2}{\Psi_{ve}(u) + \Psi_{ve}(v)}$
ve-degree sum connectivity index (χ_{ve})	$\chi_{ve} = \sum_{uv\in E}(\Psi_{ve}(u) + \Psi_{ve}(v))^{-1/2}$

https://doi.org/10.1021/acsomega.2c06287
ACS Omega 2022, 7, 45562−45573

We only study connected, undirected, and simple graphs in this work. Let Γ be a molecular graph with $\vartheta(\Gamma)$ as the vertex set, $E(\Gamma)$ as the edge set, and the degree of the υ vertex, denoted by δ_υ, being the number of distinct edges that can meet the υ vertex, and the open neighborhood of the υ vertex, represented by $N(\upsilon)$, being the set of all vertices adjoined to the υ vertex. The closed neighborhood of υ, denoted by $N[\upsilon]$, defines the union of υ vertex with open neighborhood $N(\upsilon)$ of υ vertex. The ev-degree of any edge $u\upsilon \in E(\Gamma)$ defines the total number of vertices of closed neighborhoods of the end vertices of an edge e, and the ev-degree is represented by $\Psi_{ev}(e)$. The ve-degree of every vertex $\upsilon \in \vartheta$ is the number of various edges that are linked to any vertex from the closed neighborhood of υ, indicated by $\Psi_{ve}(\upsilon)$.

MAIN RESULTS

In this paper, we have investigated the M_{ev}, $M^{\alpha}_{1,ve}$, $M^{\beta}_{1,ve}$, $M^{\beta}_{2,ve}$, R_{ve}, R_{ev}, ABC_{ve}, GA_{ve}, H_{ve}, and χ_{ve}. We have also given the closed formulas of these indices for the carbon nanocone $CNC_r[s]$. For computation, the combinational processing strategy, edge partition method, vertex partition method, data analysis procedures, degree counting method, and sum of degrees of neighbor methods are used in the calculations. Furthermore, Matlab programming is also used to perform numerical computations and verification.

Table 2. Edge Partition of $CNC_r[s]$

$(\delta_u,\delta_\upsilon)$	frequency
(2,2)	r
(2,3)	$2r(s-1)$
(3,3)	$\frac{r}{2}(s-1)(3s-2)$

Table 3. Vertex Partition of $CNC_r[s]$

δ_u	frequency
2	rs
3	$(s-1)rs$

Table 4. ev-Degree Partition for $CNC_r[s]$

$(\delta_u,\delta_\upsilon)$	ev-degree	frequency
(2,2)	4	r
(2,3)	5	$2r(s-1)$
(3,3)	6	$\frac{r}{2}(s-1)(3s-2)$

Table 5. ve-Degree Partition for $CNC_r[s]$

δ_u	ve-degree	frequency
2	5	rs
2	6	$r(s-2)$
3	7	$r(s-1)$
3	9	$r(s-1)^2$

Table 6. End Vertices ve-Degrees of Each Edge for $CNC_r[s]$

$(\delta_u,\delta_\upsilon)$	ve-degree	frequency
(2,2)	(5,5)	r
(2,3)	(5,7)	$2r$
(2,3)	(6,7)	$2r(s-2)$
(3,3)	(7,9)	$r(s-1)$
(3,3)	(9,9)	$r\left(\frac{s}{2}(3s-1)-(3s-2)\right)$

Theorem 0.1. Let $CNC_r[s]$, $r \geqslant 3$, $s \geqslant 2$ be the graph of carbon nanocones, then

$$M_{ev} = 54rs^2 - 40rs + 2r$$

$$M^{\alpha}_{1,ve} = 81rs^2 - 52rs - 40r$$

$$R_{ev} = \frac{3}{2\sqrt{6}}rs^2 + \left(\frac{2}{\sqrt{5}} - \frac{1}{\sqrt{6}} - \frac{3}{2\sqrt{6}}\right)rs + \left(\frac{1}{2} - \frac{2}{\sqrt{5}} + \frac{1}{\sqrt{6}}\right)r$$

$$M^{\beta}_{1,ve} = 27rs^2 - 21rs - 34r$$

$$M^{\beta}_{2,ve} = \frac{243}{2}rs^2 - \frac{273}{2}rs + 26r$$

$$R_{ve} = \frac{1}{6}rs^2 + \left(\frac{2}{\sqrt{42}} + \frac{1}{3\sqrt{7}} - \frac{7}{18}\right)rs + \left(\frac{2}{\sqrt{35}} + \frac{4}{42} - \frac{1}{3\sqrt{7}} - \frac{1}{45}\right)r$$

$$ABC_{ve} = \frac{2}{3}rs^2 + \left(2\sqrt{\frac{11}{42}} + \frac{\sqrt{2}}{3} - \frac{14}{9}\right)rs + \left(\frac{2\sqrt{2}}{5} + 2\sqrt{\frac{2}{7}} - 4\sqrt{\frac{11}{42}} - \frac{\sqrt{2}}{3} + \frac{8}{9}\right)r$$

$$GA_{ve} = \frac{3}{2}rs^2 + \left(4\frac{\sqrt{42}}{13} + \frac{3\sqrt{7}}{8} - \frac{5}{2}\right)rs + \left(3 - \frac{3\sqrt{7}}{8} + \frac{35}{3} - \frac{8\sqrt{42}}{13}\right)r$$

$$H_{ve} = \frac{1}{6}rs^2 + \frac{246}{5616}rs - \frac{2517}{14\,040}r$$

$$\chi_{ve} = \frac{1}{2\sqrt{2}}rs^2 + \left(\frac{2}{\sqrt{13}} + \frac{1}{4} - \frac{1}{6\sqrt{2}} - \frac{1}{\sqrt{2}}\right)rs + \left(\frac{1}{\sqrt{10}} + \frac{1}{\sqrt{3}} - \frac{4}{\sqrt{13}} - \frac{1}{4} + \frac{2}{3\sqrt{2}}\right)r$$

Proof. The carbon nanocone $CNC_r[s]$ shown in Figure 2 contains rs^2 vertices and $\frac{rs}{2}(3s-1)$ edges. Table 2 shows the three types of edges found in $CNC_r[s]$ based on degrees. The vertices of carbon nanocone $CNC_r[s]$ are either of degree two or three with rs and $(s-1)rs$ vertices shown in Table 3. Now, we compute topological indices for $CNC_r[s]$ that are based on degrees.

From Tables 4 and 5, we determine the following degree-based topological indices:

- ev-degree-based Zagreb index

https://doi.org/10.1021/acsomega.2c06287
ACS Omega 2022, 7, 45562−45573

$$
\begin{aligned}
M_{\mathrm{ev}} &= \sum_{e\in E} \Psi_{\mathrm{ev}}(e)^2 \\
&= (4)^2(r) + (5)^2(2r(s-1)) + (6)^2 \left(\frac{r}{2}(s-1)(3s-2)\right) \\
&= 16r + 50rs - 50r + 36\left(\frac{3rs^2}{2} - rs - \frac{3rs}{2} + r\right) \\
&= 16r + 50rs - 50r + 54rs^2 - 36rs - 54rs + 36r \\
&= 2r + 14rs - 54rs + 54rs^2 \\
&= 54rs^2 - 40rs + 2r
\end{aligned}
$$

- First ve-degree-based Zagreb index

$$
\begin{aligned}
M^{\alpha}_{1,\mathrm{ve}} &= \sum_{v\in\vartheta} \Psi_{\mathrm{ve}}(v)^2 \\
&= (5)^2(rs) + (6)^2(r(s-2)) + (7)^2(r(s-1)) + (9)^2(r(s-1)^2) \\
&= 25rs + 36rs - 72r + 49rs - 49rs - 49r + 81(rs^2 + r - 2rs) \\
&= 25rs + 36rs - 72r + 49rs - 49r + 81rs^2 + 81r - 162rs \\
&= 81rs^2 - 52rs - 40r
\end{aligned}
$$

- ev-degree-based Randic index

$$
\begin{aligned}
R_{\mathrm{ev}} &= \sum_{e\in E} \Psi_{\mathrm{ev}}(e)^{-1/2} \\
&= (4)^{-1/2}(r) + (5)^{-1/2}(2r(s-1)) + (6)^{-1/2} \left(\frac{r}{2}(s-1)(3s-2)\right) \\
&= \frac{r}{2} + \frac{2}{\sqrt{5}}(rs) - \frac{2}{\sqrt{5}}r + \frac{1}{\sqrt{6}}\left(\frac{3rs^2}{2} - rs - \frac{3rs}{2} + r\right) \\
&= \frac{1}{2}r + \frac{2}{\sqrt{5}}rs - \frac{2}{\sqrt{5}}r + \frac{3}{2\sqrt{6}}rs^2 - \frac{1}{\sqrt{6}}rs - \frac{3}{2\sqrt{6}}rs + \frac{1}{\sqrt{6}}r \\
&= \frac{3}{2\sqrt{6}}rs^2 + \left(\frac{2}{\sqrt{5}} - \frac{1}{\sqrt{6}} - \frac{3}{2\sqrt{6}}\right)rs + \left(\frac{1}{2} - \frac{2}{\sqrt{5}} + \frac{1}{\sqrt{6}}\right)r
\end{aligned}
$$

Using Table 6, we determine the below-mentioned ve-degree-based topological indices:

- First ve-degree-based Zagreb index

$$
\begin{aligned}
M^{\beta}_{1,\mathrm{ve}} &= \sum_{uv\in E} (\Psi_{\mathrm{ve}}(u) + \Psi_{\mathrm{ve}}(v)) \\
&= (10)(r) + (12)(2r) + (13)(2r(s-2)) + (16)(r(s-1)) + (18)r\left(\frac{s}{2}(3s-1) - (3s-2)\right) \\
&= 10r + 24r + 26rs - 52r + 16rs - 16r + 18r\left(\frac{s}{2}(3s-1) - (3s-2)\right) \\
&= 34r - 68r + 42rs + 27rs^2 - 9rs - 54rs + 36r \\
&= 27rs^2 - 21rs - 34r
\end{aligned}
$$

- Second ve-degree-based Zagreb index

$$
\begin{aligned}
M^{\beta}_{2,\mathrm{ve}} &= \sum_{uv\in E} (\Psi_{\mathrm{ve}}(u) \times \Psi_{\mathrm{ve}}(v)) \\
&= (25)(r) + (35)(2r) + (42)(2r(s-2)) + (63)(r(s-1)) + (81)r\left(\frac{s}{2}(3s-1) - (3s-2)\right) \\
&= 25r + 70r + 84r(s-2) + 63r(s-1) + 81r\left(\frac{s}{2}(3s-1) - (3s-2)\right) \\
&= 32r - 168r + 147rs + \frac{243}{2}rs^2 - \frac{81}{2}rs - 243rs + 162r \\
&= 26r - 96rs - \frac{81}{2}rs + \frac{243}{2}rs^2 \\
&= \frac{243}{2}rs^2 - \frac{273}{2}rs + 26r
\end{aligned}
$$

- ve-degree-based Randic index

https://doi.org/10.1021/acsomega.2c06287
ACS Omega 2022, 7, 45562−45573

$$
\begin{aligned}
R_{ve} &= \sum_{uv\in E} (\Psi_{ve}(u) \times \Psi_{ve}(v))^{-1/2} \\
&= (25)^{-1/2}(r) + (35)^{-1/2}(2r) + (42)^{-1/2} \\
&\quad (2r(s-2)) + (63)^{-1/2}(r(s-1)) \\
&\quad + (81)^{-1/2} r\left(\frac{s}{2}(3s-1) - (3s-2)\right) \\
&= \frac{1}{5}r + \frac{2}{\sqrt{35}}r + \frac{2}{\sqrt{42}}(r(s-2)) + \frac{1}{3\sqrt{7}} \\
&\quad (r(s-1)) + \frac{1}{9}r\left(\frac{s}{2}(3s-1) - (3s-2)\right) \\
&= \frac{1}{5}r + \frac{2}{\sqrt{35}}r + \frac{2}{\sqrt{42}}(r(s-2)) + \frac{1}{3\sqrt{7}} \\
&\quad (r(s-1)) + \frac{1}{6}rs^2 - \frac{1}{18}rs - \frac{1}{3}rs - \frac{2}{9}r \\
&= \frac{1}{6}rs^2 + \left(\frac{2}{\sqrt{42}} + \frac{1}{3\sqrt{7}} - \frac{7}{18}\right)rs \\
&\quad + \left(\frac{2}{\sqrt{35}} + \frac{4}{\sqrt{42}} - \frac{1}{3\sqrt{7}} - \frac{1}{45}\right)r
\end{aligned}
$$

- ve-degree-based atom−bond connectivity index

$$
\begin{aligned}
ABC_{ve} &= \sum_{uv\in E} \sqrt{\frac{\Psi_{ve}(u) + \Psi_{ve}(v) - 2}{\Psi_{ve}(u) \times \Psi_{ve}(v)}} \\
&= \sqrt{\frac{8}{25}}(r) + \sqrt{\frac{10}{35}}(2r) + \sqrt{\frac{11}{42}} \\
&\quad (2r(s-2)) + \sqrt{\frac{14}{63}}(r(s-1)) + \sqrt{\frac{16}{81}} \\
&\quad r\left(\frac{s}{2}(3s-1) - (3s-2)\right) \\
&= \frac{2\sqrt{2}}{5}r + 2\sqrt{\frac{2}{7}}r + \sqrt{\frac{11}{42}}(2r(s-1)) \\
&\quad + \sqrt{\frac{2}{9}}(r(s-1)) + \frac{4}{9}r\left(\frac{s}{2}(3s-1)\right. \\
&\quad \left. - (3s-2)\right) \\
&= \frac{2\sqrt{2}}{5}r + 2\sqrt{\frac{2}{7}}r + 2\sqrt{\frac{11}{42}}rs - 4\sqrt{\frac{11}{42}}r \\
&\quad + \frac{\sqrt{2}}{3}rs - \frac{\sqrt{2}}{3}r + \frac{2}{9}rs(3s-1) \\
&\quad - \frac{4}{9}r(3s-2) \\
&= \frac{2}{3}rs^2 + \left(2\sqrt{\frac{11}{42}} + \frac{\sqrt{2}}{3} - \frac{14}{9}\right)rs \\
&\quad + \left(\frac{2\sqrt{2}}{5} + 2\sqrt{\frac{2}{7}} - 4\sqrt{\frac{11}{42}} - \frac{\sqrt{2}}{3}\right. \\
&\quad \left. + \frac{8}{9}\right)r
\end{aligned}
$$

- ve-degree-based geometric−arithmetic index

$$
\begin{aligned}
GA_{ve} &= \sum\nolimits_{uv\in E} \frac{\sqrt[2]{\Psi_{ve}(u) \times \Psi_{ve}(v)}}{\Psi_{ve}(u) + \Psi_{ve}(v)} \\
&= \frac{2\sqrt{25}}{10}(r) + \frac{2\sqrt{35}}{12}(2r) + \frac{2\sqrt{42}}{13} \\
&\quad (2r(s-2)) + \frac{2\sqrt{63}}{16}(r(s-1))\frac{2\sqrt{81}}{18}r \\
&\quad \left(\frac{s}{2}(3s-1) - (3s-2)\right) \\
&= r + \frac{2\sqrt{35}}{6}r + \frac{2\sqrt{42}}{13}(2r(s-2)) \\
&\quad + \frac{\sqrt{63}}{8}(r(s-1)) + r\left(\frac{s}{2}(3s-1)\right. \\
&\quad \left. - (3s-2)\right) \\
&= r + \frac{\sqrt{35}}{3}r + \frac{4\sqrt{42}}{13}rs - \frac{8\sqrt{42}}{13}r \\
&\quad + \frac{3\sqrt{7}}{8}rs - \frac{3\sqrt{7}}{8}r + \frac{3}{2}rs^2 - \frac{1}{2}rs \\
&\quad - 3rs + 2r \\
&= \frac{3}{2}rs^2 + \left(\frac{4\sqrt{42}}{13} + \frac{3\sqrt{7}}{8} - \frac{5}{2}\right)rs \\
&\quad + \left(3 - \frac{3\sqrt{7}}{8} + \frac{\sqrt{35}}{3} - \frac{8\sqrt{42}}{13}\right)r
\end{aligned}
$$

- ve-degree-based harmonic index

$$
\begin{aligned}
H_{ve} &= \sum_{uv\in E} \frac{2}{\Psi_{ve}(u) + \Psi_{ve}(v)} \\
&= \frac{2}{10}(r) + \frac{2}{12}(2r) + \frac{2}{13}(2r(s-2)) \\
&\quad + \frac{2}{16}(r(s-1)) + \frac{2}{18}r\left(\frac{s}{2}(3s-1)\right. \\
&\quad \left. - (3s-2)\right) \\
&= \frac{1}{5}r + \frac{1}{3}r + \frac{4}{13}rs - \frac{8}{13}r + \frac{1}{8}rs - \frac{1}{8}r \\
&\quad + \frac{1}{9}r\left(\frac{s}{2}(3s-1) - (3s-2)\right) \\
&= \frac{1}{6}rs^2 + \left(\frac{4}{13} + \frac{1}{8} - \frac{1}{3} - \frac{1}{18}\right)rs \\
&\quad + \left(\frac{1}{5} + \frac{1}{3} - \frac{8}{13} - \frac{1}{8} + \frac{2}{9}\right)r \\
&= \frac{1}{6}rs^2 + \frac{246}{5616}rs - \frac{2517}{14\,040}r
\end{aligned}
$$

- ve-degree-based sum connectivity index

https://doi.org/10.1021/acsomega.2c06287
ACS Omega 2022, 7, 45562−45573

$$\chi_{ve} = \sum_{uv\in E} (\Psi_{ve}(u) + \Psi_{ve}(v))^{-1/2}$$

$$= (10)^{-1/2}(r) + (12)^{-1/2}(2r) + (13)^{-1/2}(2r(s-2)) + (16)^{-1/2}(r(s-1)) + (18)^{-1/2}r\left(\frac{s}{2}(3s-1) - (3s-2)\right)$$

$$= \frac{1}{\sqrt{10}}r + \frac{1}{\sqrt{3}}r + \frac{2}{\sqrt{13}}rs - \frac{4}{\sqrt{13}}r + \frac{1}{4}rs - \frac{1}{4}r + \frac{1}{2\sqrt{2}}rs^2 - \frac{1}{6\sqrt{2}}rs - \frac{1}{\sqrt{2}}rs + \frac{2}{3\sqrt{2}}r$$

$$= \frac{1}{2\sqrt{2}}rs^2 + \left(\frac{2}{\sqrt{13}} + \frac{1}{4} - \frac{1}{6\sqrt{2}} - \frac{1}{\sqrt{2}}\right)rs + \left(\frac{1}{\sqrt{10}} + \frac{1}{\sqrt{3}} - \frac{4}{\sqrt{13}} - \frac{1}{4} + \frac{2}{3\sqrt{2}}\right)r$$

NUMERICAL RESULTS AND DISCUSSION

In this section, for different values of r and s, we present numerical findings (see Tables 7 and 8) and graphical representations (see Figures 4−13) for the above-computed ev-degree- and ve-degree-based topological indices for the molecular structure of carbon nanocone $CNC_r[s]$.

Here, we consider $r = 3-5$ and $s = 2-4$ for numerical results and graph representations but results are applicable for $r \geq 3$ and $s \geq 2$. Moreover, these numerical results and plots for the molecular structure $CNC_r[s]$ are computed by utilizing Matlab programming.

Table 7. Numerical Computation for $CNC_r[s]$

$r[s]$	M_{ev}	$M^{\alpha}_{1,ve}$	R_{ev}	$M^{\beta}_{1,ve}$	$M^{\beta}_{2,ve}$
3[2]	414	540	6.63	96	717
3[3]	1104	1599	15.42	438	2130
3[4]	2118	3144	27.87	942	4272
4[2]	552	720	8.84	128	956
4[3]	1472	2132	20.56	584	2840
4[4]	2824	4192	37.16	1256	5696
5[2]	690	900	11.05	160	1195
5[3]	1840	2665	25.70	730	3550
5[4]	3530	5240	46.45	1570	7120

Table 8. Numerical Computation for $CNC_r[s]$

$r[s]$	R_{ve}	ABC_{ve}	GA_{ve}	H_{ve}	χ_{ve}
3[2]	3.048	4.542	49.950	1.641	19.056
3[3]	5.583	14.253	73.890	4.170	24.234
3[4]	9.078	27.924	106.83	7.659	31.512
4[2]	4.064	6.056	66.60	2.188	25.408
4[3]	7.444	19.004	98.52	5.560	32.312
4[4]	12.104	37.232	142.44	10.212	42.016
5[2]	5.080	7.570	83.25	2.735	31.760
5[3]	9.305	23.755	123.15	6.950	40.390
5[4]	15.130	46.540	178.05	12.765	52.5200

All computed topological indices exceed with the exceeding value of r and s, as seen in Tables 7 and 8, and Figures 4−13 also show relationships between several topological indices for various values of r and s.

The Zagreb type of indices was discovered by analyzing the total π-electron energy of molecules.[23] It was also apparent that the first and second Zagreb indices represent the degree of branching in the molecular structure and are therefore responsible for the overall decrease in π-electron energy with increased branching. As a result, the total π-electron energy for the carbon nanocone $CNC_r[s]$ decreases with increasing values of r and s.

The Randic index was used to quantitatively characterize the degree of molecular branching. The degree of branching of the molecular skeleton is a key determinant for various molecular attributes, such as boiling points of hydrocarbons and the retention volumes and the analysis of chemical similarity of molecular compounds.[30] In addition, the Randic index was utilized to calculate the Kovats constants and the boiling points of molecules. According to Bollobas and Erdos[39,40] for a minimum value of $R(\Gamma)$, there is minimum degree $\delta(\Gamma)$ for graphs Γ. This implies that higher is the value of branching degree, i.e., r and s, higher the Randic index for the carbon nanocone $CNC_r[s]$.

The geometric−arithmetic index has been found to have greater predictive power than the Randic connection index.[32] Since this index is related to the degree of the vertices of the graph, then with the increase of edges in the graph, the GA index increases. As a result, the GA index for the carbon nanocone $CNC_r[s]$ increases as r and s are increased.

The atom−bond connectivity (ABC) index is particularly useful for the calculation of the strain energy of cycloalkanes as well as the stability of linear and branched alkanes.[32] In particular, ABC must increase if a new edge is added to G.[41] By means of this result, we analyze that the carbon nanocone $CNC_r[s]$ in the current work has an improved ABC index due to the improvement of r and s.

Conclusions. Topological indices are utilized to determine the core topologies of the molecular structure of carbon nanocone $CNC_r[s]$. In this study, we utilized various combinational processing strategies to obtain results for ev-degree- and ve-degree-based topological indices such as M_{ev}, $M^{\alpha}_{1,ve}$, $M^{\beta}_{1,ve}$, $M^{\beta}_{2,ve}$, R_{ve}, R_{ev}, ABC_{ve}, GA_{ve}, H_{ve}, and χ_{ve} for the molecular structure of carbon nanocone $CNC_r[s]$. Furthermore, Matlab programming is used to perform numerical computations and graph plotting. These findings will help to predict and model the physicochemical features of chemical substances that have not been thoroughly investigated. It can be interesting to compute these ev-degree- and ve-degree-based topological indices of some other molecular structures and networks for further studies. It can also be interesting to calculate distance-based topological indices of understudied nanocones.

APPENDIX MATLAB CODING

Matlab coding steps for plotting 3D surface graphs of topological indices:

- $r = r_1: r_2;$ → set the range of x-axis
- $s = s_1: s_2;$ → set the range of y-axis
- $[X, Y]$ = meshgrid(r,s) → matrix type, the value of r, s appears on the worksheet

https://doi.org/10.1021/acsomega.2c06287
ACS Omega 2022, 7, 45562−45573

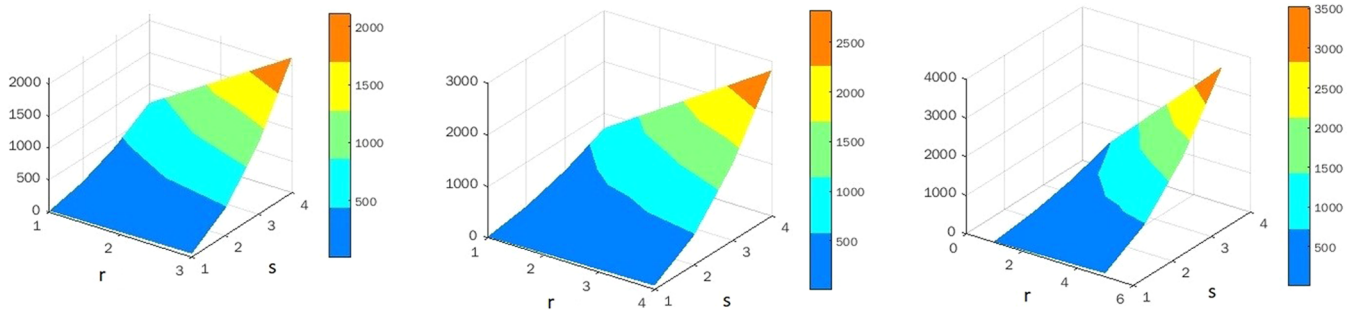

Figure 4. Plot for the M_{ev} for r = 3−5 and s = 2−4.

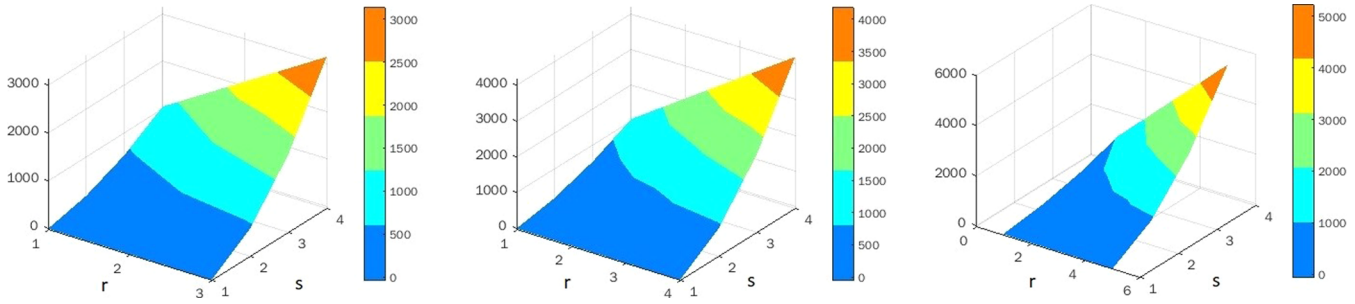

Figure 5. Plot for the $M^{\alpha}_{1,ve}$ for r = 3−5 and s = 2−4.

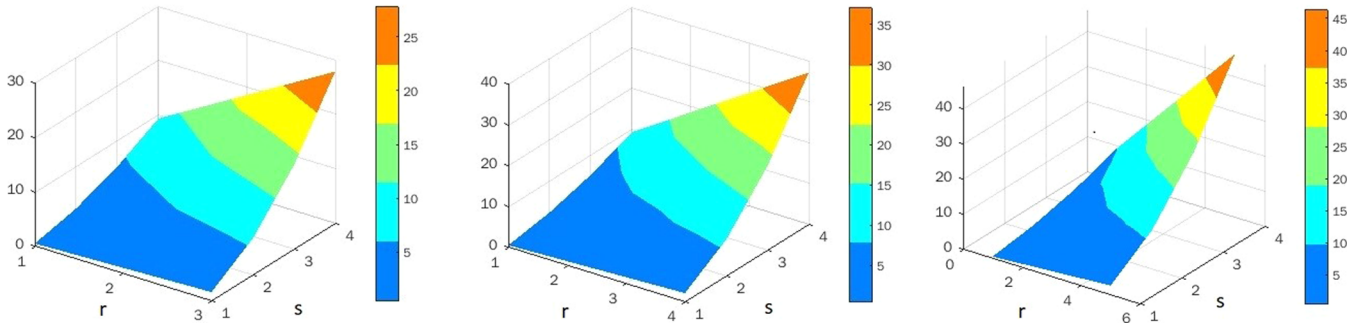

Figure 6. Plot for the R_{ev} for r = 3−5 and s = 2−4.

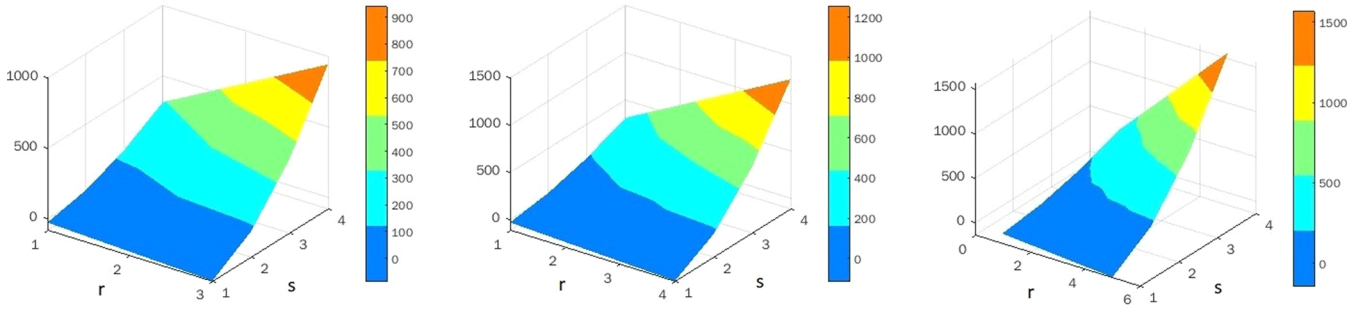

Figure 7. Plot for the $M^{\beta}_{1,ve}$ for r = 3−5 and s = 2−4.

- Z = a*X.*Y.^{2} − b*X.*Y + 2*X → polynomial from which we find the value of Z and set the range of z-axis
- mesh(X,Y,Z) → by finding the numerical values of the function, the meshgrid figure appears on the worksheet
- figure → space appears for the figure
- surf(X,Y,Z) → a surface graph plot on the Matlab worksheet
- $x$label(r) → 'r' labeled on the x-axis
- $y$label(s) → 's' labeled on the y-axis
- view ([35,30]) → rotate the 3D graph according to your choice
- shading interp → shading the plot surface and disappearing of the grids shown on it % get rid of black lines in the surface plot
- colorbar → colorbar appears on the left/right side of the plot %adds a colorbar that acts as a legend for colors
- colormap(jet(5))\winter\summer → coloring the plotting surface as per your choice

Example

https://doi.org/10.1021/acsomega.2c06287
ACS Omega 2022, 7, 45562−45573

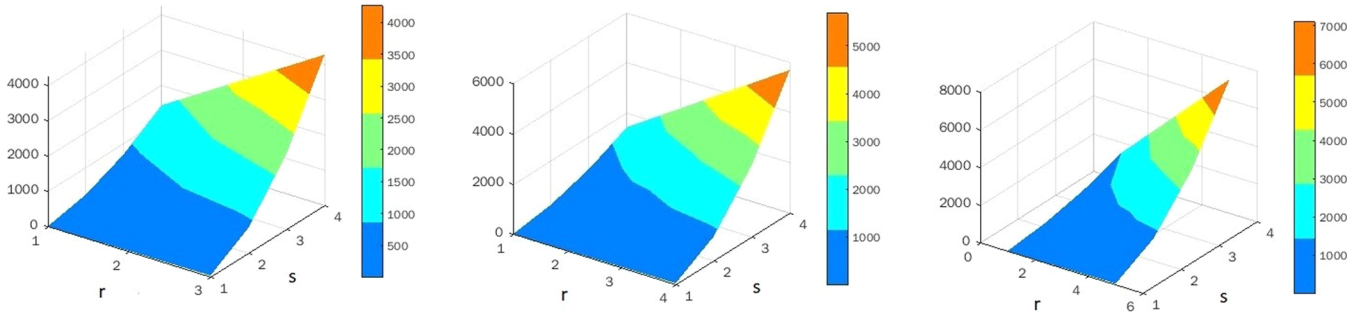

Figure 8. Plot for the $M_{2,ve}^{\beta}$ for r = 3−5 and s = 2−4.

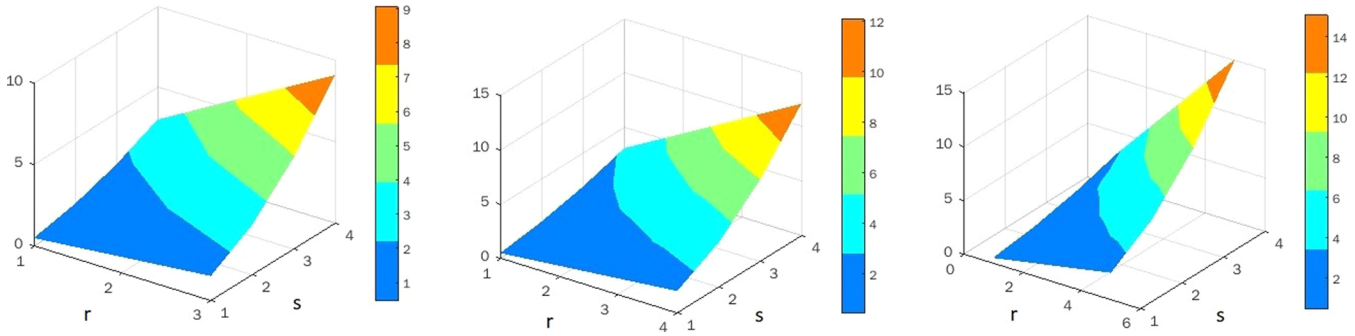

Figure 9. Plot for the R_{ve} for r = 3−5 and s = 2−4.

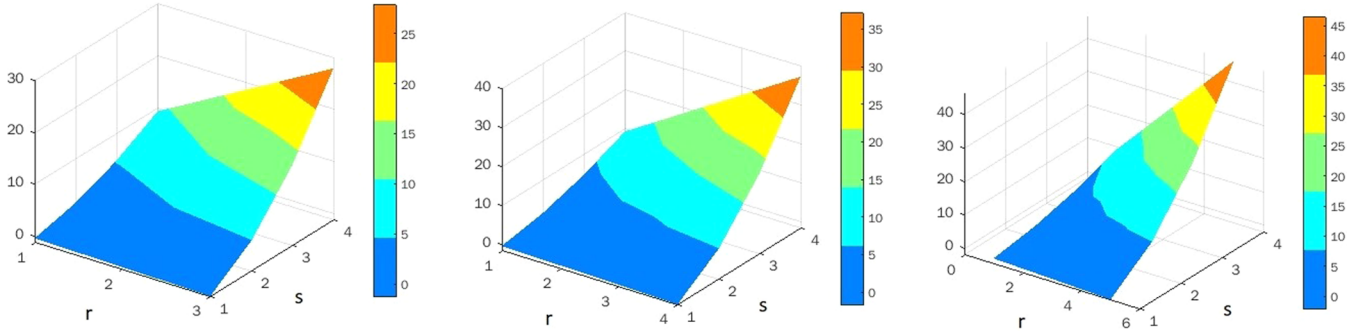

Figure 10. Plot for the ABC_{ve} for r = 3−5 and s = 2−4.

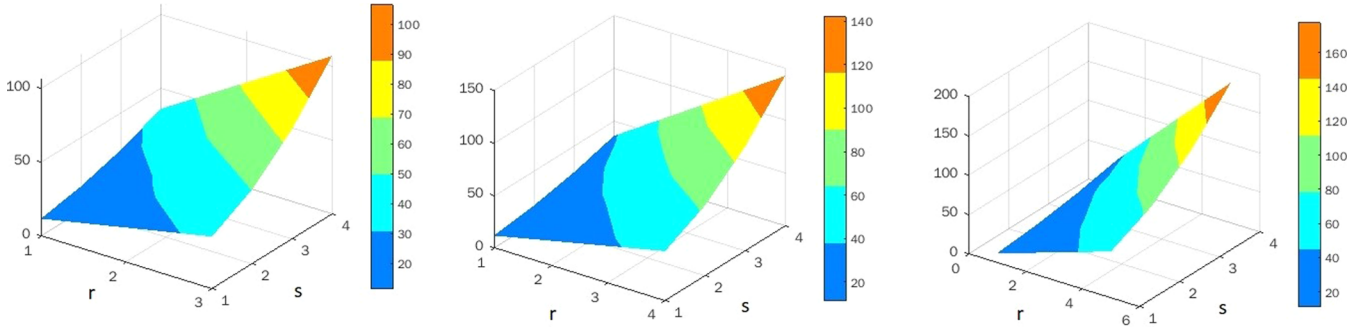

Figure 11. Plot for the GA_{ve} for r = 3−5 and s = 2−4.

https://doi.org/10.1021/acsomega.2c06287
ACS Omega 2022, 7, 45562−45573

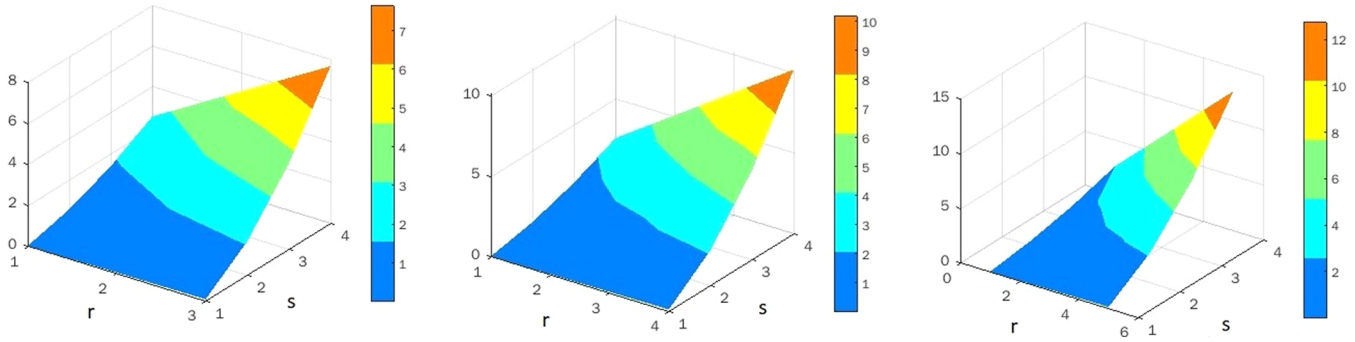

Figure 12. Plot for the H_{ve} for r = 3−5 and s = 2−4.

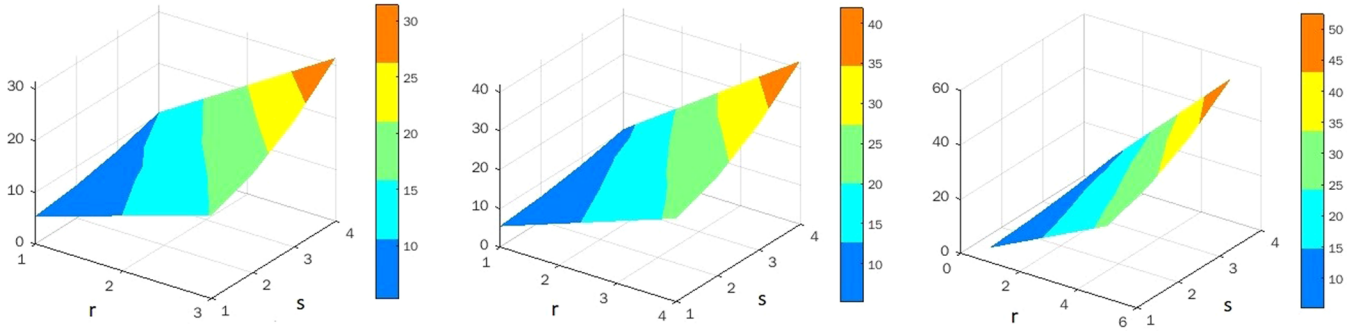

Figure 13. Plot for the χ_{ve} for r = 3−5 and s = 2−4.

$r = 1{:}\ 3;$

$s = 1{:}\ 4;$

$$[X,\ Y] = \text{meshgrid}(r,\ s)\begin{pmatrix}1 & 2 & 3\\ 1 & 2 & 3\\ 1 & 2 & 3\end{pmatrix}\begin{pmatrix}1 & 1 & 1\\ 2 & 2 & 2\\ 3 & 3 & 3\\ 4 & 4 & 4\end{pmatrix}$$

$$Z = 54{}^{*}X.\ {}^{*}Y.^{2} - 40{}^{*}X.\ {}^{*}Y + 2{}^{*}X$$

$$\begin{pmatrix}16 & 32 & 48\\ 138 & 276 & 414\\ 368 & 736 & 1104\\ 706 & 1412 & 2118\end{pmatrix}$$

mesh(*X*,*Y*,*Z*)
figure:
surf(*X*,*Y*,*Z*)
*x*label(*r*)
*y*label(*s*)
view([35, 30])
shading interp
%gets rid of black lines in the surface plot
colorbar
%adds a colorbar that acts as a legend for colors
colormap(jet(5))\winter\summer

■ ASSOCIATED CONTENT

Data Availability Statement

Data sharing is not applicable to this article as no data set was generated or analyzed during the current study.

■ AUTHOR INFORMATION

Corresponding Author

Vijay Kumar Bhat − *School of Mathematics, Shri Mata Vaishno Devi University, Katra 182320 Jammu and Kashmir, India;* orcid.org/0000-0001-8423-9067; Email: vijaykumarbhat2000@yahoo.com

Authors

Karnika Sharma − *School of Mathematics, Shri Mata Vaishno Devi University, Katra 182320 Jammu and Kashmir, India*

Sunny Kumar Sharma − *School of Mathematics, Shri Mata Vaishno Devi University, Katra 182320 Jammu and Kashmir, India*

Complete contact information is available at: https://pubs.acs.org/10.1021/acsomega.2c06287

Author Contributions

All of the authors have equally contributed to the final manuscript.

Funding

Karnika Sharma has received research support from the Department of Science and Technology (DST), Government of India (INSPIRE Fellowship IF180978).

Notes

The authors declare no competing financial interest.

Novelty Statement: The ev-degree- and ve-degree-based topological indices of several molecular structures have recently been computed. Correlating and predicting the characteristics of a wide range of molecular structures is one of the most challenging problems in chemistry. Numerous topological indices have been developed to better understand the physical properties, chemical reactivity, and biological activity of these chemical molecular structures. The ev- and ve-degree TIs for molecular graphs are a recently developed field

https://doi.org/10.1021/acsomega.2c06287
ACS Omega 2022, 7, 45562−45573

that translates each chemical structure into a real number and acts as a description of the molecule under test. As far as we are aware, no research has been published on the ev-degree- and ve-degree-based TIs of carbon nanocones. In this work, we compute the generalized carbon nanocones, $CNC_r[s]$. Furthermore, we find numerical computations for certain types of nanocones and use Matlab programming to depict these numerical results.

■ ACKNOWLEDGMENTS

The authors would like to express their sincere gratitude to the referees for their careful reading of this manuscript and for all of their insightful comments/criticism, which have given the present shape to the manuscript.

■ ADDITIONAL NOTE

[†]On Degree-Based Topological Indices of Carbon Nanocones.

■ REFERENCES

(1) Klein, D. J.; Balaban, A. T. The eight classes of positive-curvature graphitic nanocones. *J. Chem. Inf. Model.* **2006**, *46*, 307−320.
(2) Sagar, T. C.; Chinthapenta, V.; Horstemeyer, M. V. Effect of defect guided out of-plane deformations on the mechanical properties of graphene. *Fullerenes, Nanotubes, Carbon Nanostruct.* **2021**, *29*, 83−99.
(3) Karousis, N.; Suarez-Martinez, I.; Ewels, C. P.; Tagmatarchis, N. Structure, properties, functionalization, and applications of carbon nanohorns. *Chem. Rev.* **2016**, *116*, 4850−4883.
(4) Brinkmann, G.; Van Cleemput, N. Classification and generation of nanocones. *Discret. Appl. Math.* **2011**, *159*, 1528−1539.
(5) Justus, C.*Boundaries of Triangle-Patches and the Expander Constant of Fullerenes*; Universität Bielefeld, 2007.
(6) Sharma, S. K.; Raza, H.; Bhat, V. K. Computing edge metric dimension of one-pentagonal carbon nanocone. *Front. Phys.* **2021**, *9*, No. 749166.
(7) Arockiaraj, M.; Clement, J.; Balasubramanian, K. Topological troperties of carbon nanocones. *Polycyclic Aromat. Compd.* **2018**, *40*, 1332−1346.
(8) Sharma, K.; Bhat, V. K.; Sharma, S. K. Edge metric dimension and edge basis of one-heptagonal carbon nanocone networks. *IEEE Access.* **2022**, *10*, 29558−29566.
(9) Mortazavi, B.; Javvaji, B.; Shojaei, F.; Rabczuk, T.; Shapeev, A. V.; Zhuang, X. Exceptional piezoelectricity, high thermal conductivity and stiffness and promising photocatalysis in two-dimensional $MoSi_2N_4$ family confirmed by first-principles. *Nano Energy* **2021**, *82*, No. 105716.
(10) Javvaji, B.; Zhuang, X.; Rabczuk, T.; Mortazavi, T. Machine-learning-based exploration of bending flexoelectricity in novel 2D van der waals bilayers. *Adv. Energy Mater.* **2022**, *12*, No. 2201370.
(11) Jahanbani, A. On topological indices of carbon nanocones and nanotori. *Int. J. Quantum Chem.* **2019**, *120*, 1−15.
(12) Zobair, M. M.; Malik, M. A.; Shaker, H. Eccentricity-based topological invariants of tightest nonadjacently configured stable pentagonal structure of carbon nanocones. *Int. J. Quantum Chem.* **2021**, *121*, No. e26807.
(13) Arockiaraj, M.; Klavzar, S.; Clement, J.; Mushtaq, S.; Balasubramanian, K. Edge distance-based topological indices of strength-weighted graphs and their application to coronoid systems, carbon nanocones and SiO2 nanostructures. *Mol. Inf.* **2019**, *38*, No. 1900039.
(14) Rauf, A.; Naeem, M.; Bukhari, S. U. Quantitative structure−property relationship of ev-degree and ve-degree based topological indices: physico-chemical properties of benzene derivatives. *Int. J. Quantum Chem.* **2022**, *122*, No. e26851.
(15) Rouvray, D. H.; Tatong, W. Novel applications of topological indices: 1. Prediction of the ultrasonic sound velocity in alkanes and alcohols. zeitschrift fur naturforschung A: *J. Phys. Sci.* **1986**, *41*, 1238−1244.
(16) Hanson, M. P.; Rouvray, D. H. Novel applications of topological indices. 2. Prediction of the threshold soot index for hydrocarbon fuels. *J. Phys. Chem. A* **1987**, *91*, 2981−2985.
(17) Wiener, H. Structural determination of paraffin boiling points. *J. Am. Chem. Soc.* **1947**, *69*, 17−20.
(18) Gutman, I.; Milovanovic, E.; Milovanovic, I. Beyond the zagreb indices. *AKCE Int. J. Graphs Comb.* **2020**, *17*, 74−85.
(19) Shanmukha, M. C.; Basavarajappa, N. S.; Shilpa, K. C.; Usha, A. Degree-based topological indices on anticancer drugs with QSPR analysis. *Heliyon* **2020**, *6*, No. e04235.
(20) Havare, Ö. Ç. Quantitative structure analysis of some molecules in drugs used in the treatment of COVID-19 with topological indices. *Polycyclic Aromat. Compd.* **2022**, *42*, 5249−5260.
(21) Kirmani, S. A. K.; Ali, P.; Azam, F. Topological indices and QSPR/QSAR analysis of some antiviral drugs being investigated for the treatment of COVID-19 patients. *Int. J. Quantum Chem.* **2021**, *121*, No. e26594.
(22) Platt, J. R. Absolute absorption intensities of alkyl benzenes. *J. Chem. Phys.* **1947**, *15*, 419−420.
(23) Gutman, I.; Trinajstić, N. Graph theory and molecular orbitals. Total π-electron energy of alternant hydrocarbons. *Chem. Phys. Lett.* **1972**, *17*, 535−538.
(24) Zhong, L. The harmonic index for graphs. *Appl. Math. Lett.* **2012**, *25*, 561−566.
(25) Ediz, S. Predicting some physicochemical properties of octane isomers, a topological approach using ev-degree and ve-degree zagreb indices. *Int. J. Syst. Sci. Appl. Math.* **2017**, *2*, 87−97.
(26) Peters, K. W. J.Theoretical and algorithmic results on domination and connectivity (nordhaus-gaddum, gallai type results, max-min relationships, linear time, series-parallel1987, 2020.
(27) Jena, S. K.; Das, G. K. Vertex-edge domination in unit disk graphs. *Discret. Appl. Math.* **2022**, *319*, 351−361.
(28) Chellali, M.; Haynes, T. W.; Hedetniemi, S. T.; Lewis, T. M. On ve-Degrees and ev-Degrees in graphs. *Discrete Math.* **2017**, *340*, 31−38.
(29) Horoldagva, B.; Das, K. C.; Selenge, T. A. On ve-degree and ev-degree of graphs. *Discrete Optim.* **2019**, *31*, 1−7.
(30) Ediz, S. A new tool for QSPR researches, ev-degree randic index. *Celal Bayar Univ. J. Sci.* **2017**, *13*, 615−618.
(31) Sahin, B.; Ediz, S. On ev-degree and ve-degree topological indices. *Iran. J. Math. Chem.* **2018**, *9*, 263−277.
(32) Cancan, M.; Ediza, S.; Farahanib, M. R. On ve-degree atom-bond connectivity, sum-connectivity, geometric-arithmetic and harmonic indices of copper oxide. *Eurasian Chem. Commun.* **2020**, *2*, 641−645.
(33) Rauf, A.; Ishtiaq, M.; Siddiqui, M. K. Topological study of hydroxychloroquine conjugated molecular structure used for novel coronavirus (COVID-19) treatment. *Polycyclic Aromat. Compd.* **2022**, *42*, 3792−3808.
(34) Rauf, A.; Ishtiaq, M.; Siddiqui, M. K.; Andleeb, R. Topological properties of doxorubicin conjugated PEG-PAsp copolymer molecular structure used in cancer treatment. *Polycyclic Aromat. Compd.* **2022**, *42*, 1596−1609.
(35) Zhang, J.; Siddiqui, M. K.; Rauf, A.; Ishtiaq, M. On ve-degree and ev-degree based topological properties of single walled titanium dioxide nanotube. *J. Clust. Sci.* **2021**, *32*, 821−832.
(36) Sharma, K.; Bhat, V. K. On topological descriptors of polycyclic aromatic benzenoid systems. *Polycyclic Aromat. Compd.* **2022**, 1−20.
(37) Chu, Y. M.; Siddiqui, M. K.; Muhammad, F. H.; et al. On ve-degree and ev-degree based topological properties of H-naphtalenic nanotube. *Polycyclic Aromat. Compd.* **2022**, *42*, 2420−2432.
(38) Cai, Z. Q.; Rauf, A.; Ishtiaq, M.; Siddiqui, M. K. On ve-degree and ev-degree based topological properties of silicon carbide Si2C3-II[p,q]. *Polycyclic Aromat. Compd.* **2022**, *42*, 593−607.
(39) Delorme, C.; Favaron, O.; Rautenbach, D. On the randic index. *Discrete Math.* **2002**, *257*, 29−38.

https://doi.org/10.1021/acsomega.2c06287
ACS Omega 2022, 7, 45562−45573

(40) Du, Z.; Zhou, B.; Trinajstic, N. On geometric-arithmetic indices of (molecular) trees, unicyclic graphs and bicyclic graphs. *MATCH Commun. Math. Comput. Chem.* **2011**, *66*, 681−697.
(41) Das, K. C.; Rodriguez, J. M.; Sigarreta, J. M. On the generalized ABC index of graphs. *MATCH Commun. Math. Comput. Chem.* **2022**, *87*, 147−169.

https://doi.org/10.1021/acsomega.2c06287
ACS Omega 2022, 7, 45562−45573